Quantum Mechanical Exchange Coupling in Iridium Trihydride Complexes

D. Michael Heinekey,* Amber S. Hinkle, and John D. Close

Contribution from the Department of Chemistry, University of Washington, Box 351700, Seattle, Washington 98195-1700

Received June 29, 1995[⊗]

Abstract: Cationic trihydride complexes of the form $[(\eta\text{-}C_5R_5)Ir(L)H_3]BF_4$ (R = H, Me; L = various phosphines) have been studied. The ^{1}H NMR spectra of these complexes at low temperature display line patterns in the hydride region consistent with AB_2X or A_2BX spin systems (X = ^{31}P). The values for the H_A-H_B coupling constant (J_{AB}) derived by computer simulation of the observed spectra are large, ranging from 20−830 Hz. In general, J_{AB} is inversely proportional to the basicity of the ligand L and strongly temperature dependent. These unusual coupling constants have been attributed to quantum mechanical exchange coupling of the hydride ligands. All of the complexes have been partially deuterated and tritiated at the hydride sites and studied by both ^{1}H and ^{3}H NMR spectroscopy. In contrast to J_{AB}, the values of J_{HT} and J_{TT} are independent of temperature. The observed values for J_{HT} have been used to ascertain the contribution of the magnetic H−H coupling to J_{AB}. The contributions of the exchange coupling to J_{AB} have been derived and the corresponding temperature dependency accurately modeled. Significant isotope effects on the values of J_{AB} and the hydride chemical shifts were observed upon tritium and deuterium substitution. The barriers for thermally activated hydride site exchange have also been determined. No appreciable kinetic isotope effects on the thermally activated rearrangement process were observed upon substitution of D and T into the hydride sites. These results are interpreted in terms of a new two-dimensional model for quantum mechanical exchange coupling of the hydrides in these cationic complexes.

Introduction

Transition-metal hydride complexes have been the focus of considerable research because of their prominent role in many catalytic hydrogenation processes.[1] In 1984, conclusive evidence of the first intact H_2 molecule bound to a metal center was reported.[2] Subsequently a number of dihydrogen complexes have been reported, including several polyhydrides believed to contain both dihydrogen and hydride ligands.[3] Some dihydrogen complexes also exist in equilibrium with their dihydride isomers.[3] In recent years yet another class of transition-metal hydrogen complexes has been defined, those which are structurally characterized as hydrides, but in which the hydride ligands undergo quantum mechanical exchange coupling. While a number of such complexes have now been reported,[4−18] only a preliminary understanding of the corresponding quantum mechanical exchange coupling interactions has been attained to date.

Transition-metal hydride complexes represent the first example of a quantum mechanical exchange interaction between massive particles at high temperatures. In contrast, thorough studies have been made of quantum mechanical exchange coupling in solid helium which gives rise to anomalies in the solid state ^{3}He NMR spectra.[19] A surface integral expression to describe quantum mechanical exchange coupling in the ^{3}He/^{4}He system has been developed.[19] In 1973, Landesman modified the surface integral for helium to describe any pair of particles undergoing ground state, quantum mechanical exchange coupling.[20] In 1990, Zilm and Heinekey reported an adaptation of the Landesman results, which quantitatively models the quantum mechanical exchange coupling observed in certain transition-metal hydrides.[7,8]

Quantum mechanical exchange coupling has been proposed to explain large, temperature dependent H−H couplings apparent in the proton (^{1}H) NMR spectra of various transition-metal hydrides.[7,8] The magnitude of these temperature dependent couplings is highly variable, ranging from tens to thousands of hertz. The magnitudes seem to depend on both the identity

⊗ Abstract published in *Advance ACS Abstracts,* May 1, 1996.

(1) James, B. R. *Homogeneous Hydrogenation*; Wiley: New York, 1973.
(2) Kubas, G. J.; Ryan, R. R.; Swanson, B. I.; Vergamini, P. J.; Wasserman, H. J. *J. Am. Chem. Soc.* **1984**, *106*, 451−452.
(3) For a recent review see: Heinekey, D. M.; Oldham, W. J., Jr. *Chem. Rev.* **1993**, *93*, 913−926.
(4) Heinekey, D. M.; Payne, N. G.; Schulte, G. K. *J. Am. Chem. Soc.* **1988**, *110*, 2303−2305.
(5) Zilm, K. W.; Heinekey, D. M.; Millar, J. M.; Payne, N. G.; Demou, P. J. *J. Am. Chem. Soc.* **1989**, *111*, 3088−3089.
(6) Heinekey, D. M.; Payne, N. G.; Sofield, C. D. *Organometallics* **1990**, *9*, 2643−2645.
(7) Heinekey, D. M.; Millar, J. M.; Koetzle, T. F.; Payne, N. G.; Zilm, K. W. *J. Am. Chem. Soc.* **1990**, *112*, 909−919.
(8) Zilm, K. W.; Heinekey, D. M.; Millar, J. M.; Payne, N. G.; Neshyba, S. P.; Duchamp, J. C.; Szczyrba, J. *J. Am. Chem. Soc.* **1990**, *112*, 920−929.
(9) Heinekey, D. M.; Harper, T. G. P. *Organometallics* **1991**, *10*, 2891−2895.
(10) Heinekey, D. M. *J. Am. Chem. Soc.* **1991**, *113*, 6074−6077.
(11) Arliguie, T.; Chaudret, B.; Devillers, J.; Poilblanc, R. *C. R. Acad. Sci., Ser. II* **1987**, *305*, 1523−1526.
(12) Antiñolo, A.; Chaudret, B.; Commenges, G.; Fajardo, M.; Jalón, F.; Morris, R. H.; Otero, A.; Schweitzer, C. T. *J. Chem. Soc., Chem. Commun.* **1988**, 1210−1212.
(13) Arliguie, T.; Border, C.; Chaudret, B.; Devillers, J.; Poilblanc, R. *Organometallics* **1989**, *8*, 1308−1314.
(14) Arliguie, T.; Chaudret, B.; Jalón, F.; Otero, A.; Lopez, J. A.; Lahoz, F. J. *Organometallics* **1991**, *10*, 1888−1896.
(15) Antinolo, A.; Carrillo, F.; Fernandez-Baeza, J.; Otero, A.; Fajardo, M.; Chaudret, B. *Inorg. Chem.* **1992**, *31*, 5156−5157.
(16) Chaudret, B.; Limbach, H. H.; Moise, C. *C. R. Acad. Sci., Ser II* **1992**, *315*, 533−536.
(17) Antiñolo, A.; Carrillo, F.; Chaudret, B.; Fernandez-Baeza, J.; Lafranchi, M.; Limbach, H. H.; Maurer, M.; Otero, A.; Pellinghelli, M. A. *Inorg. Chem.* **1994**, *33*, 5163−5164.
(18) Gusev, D. G.; Kuhlman, R.; Sini, G.; Eisenstein, O.; Caulton, K. G. *J. Am. Chem. Soc.* **1994**, *116*, 2685−2686.
(19) Guyer, R. A.; Richardson, R. C.; Zane, L. E. *Rev. Mod. Phys.* **1971**, *43*, 532−600.
(20) Landesman, A. *Ann. Phys.* (Fr.) **1973**, *8*, 53−79.

S0002-7863(95)02142-1 CCC: $12.00

and charge of the metal center, and they are inversely proportional to the basicity[21] of the coligands in the complexes. We have proposed that the principal cause of this quantum interaction is a soft vibrational potential allowing substantial delocalization of the hydrides in the molecules.[7,8] There is now more extensive evidence to strongly support this model for quantum mechanical exchange coupling in transition-metal hydrides.

A different approach based on computational studies has been recently reported by Lledos and co-workers.[22] For the model compound $[CpIr(PH_3)H_3]^+$, ab initio calculations were used to build up a three-dimensional potential energy surface with particular emphasis on the consequences of hydride ligand motions. A transition state with a short H−H distance was found to be involved in the hydride permutation process, but no intermediate was found. Quantum mechanical exchange was treated in terms of a one-dimensional tunneling model. A nonzero coupling in the ground state was calculated, and the temperature dependence of the coupling was modeled by including vibrational excitation. As discussed below, these results are qualitatively in good agreement with experimental data, but there are some discrepancies when a quantitative comparison is made.

Eisenstein and co-workers have proposed a slightly different description for quantum mechanical exchange coupling in hydride complexes.[23] Ab initio calculations on complexes of the form $OsH_3X(PH_3)_2$ (X = Cl or I) lead to a model involving simultaneous vibrational and correlated rotational motions of the hydride ligands which mediate the exchange coupling.

An alternative explanation for these large, temperature dependent couplings has been proposed by Limbach, Chaudret, and co-workers. In this model, an equilibrium is postulated between a ground state hydride complex and a thermally accessible dihydrogen complex, in which rotational tunneling gives rise to the anomalous behavior detected by ^{1}H NMR spectroscopy.[24]

This model is plausible, since formation of a dihydrogen complex is generally favored by less electron density at the metal center. The magnitudes of the temperature dependent H−H couplings increase with decreasing electron density at the hydride sites. Observed trends show that the couplings increase in going from neutral to cationic complexes, from third row to second row metals and as the basicity of the coligands decreases.[4−18] Threse trends are consistent with enhanced population of a dihydrogen species leading to exchange coupling. In this paper we have attempted to distinguish between the various explanations for large, temperature dependent H−H couplings within some transition-metal hydride complexes.

We have previously reported a study of quantum mechanical exchange coupling within a series of iridium cations of the form $[(\eta\text{-}C_5H_5)Ir(L)H_3]BF_4$.[7,8] These complexes are best described structurally in terms of a capped pseudo square pyramidal geometry, with the cyclopentadienyl ligand capping, as shown below.

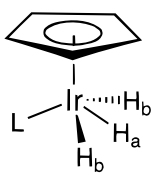

Here we will expand upon the data we have previously reported and relate our studies of the pentamethylcyclopentadienyl (Cp*) analogs of these cations. Tritium substitution and tritium (^{3}H) NMR studies have allowed determination of the separate contributions of the magnetic coupling and the exchange coupling to the observed H−H couplings. We will also describe how the experimental data lends itself to a two-dimensional model of quantum mechanical exchange coupling in these systems.

Experimental Section

General Methods. All syntheses and chemical manipulations were conducted under a nitrogen or argon atmosphere by standard Schlenk, drybox, or vacuum line techniques, unless otherwise stated. Elemental analyses were performed by Canadian Microanalytical Service Ltd. ^{1}H NMR spectra were obtained on Bruker AC-200, AF-300, and WM-500 MHz spectrometers. Chemical shifts are recorded in parts per million (ppm) relative to residual protio solvent or tetramethylsilane (TMS) $\delta = 0.00$ ppm, as noted. ^{3}H NMR spectra were obtained on a Bruker WM-500 spectrometer at 533 MHz with a Cryomagnetics tritium probe. ^{3}H chemical shifts were referenced to a fixed reference obtained from ^{1}H NMR spectra of the same sample.

Variable-temperature (VT) ^{1}H and ^{3}H NMR experiments were performed with a Bruker B-VT1000 controller with a copper/constantan thermocouple and nitrogen gas run through a copper coil immersed in liquid nitrogen to cool the sample chamber. All temperatures were calibrated by using ^{1}H chemical shifts of pure methanol[25] and a copper/constantan thermocouple inserted into the NMR probe sample chamber. The ^{1}H NMR probe was designed by Cryomagnetics specifically for low temperature studies. Simulations of NMR spectra were obtained on a Macintosh Quadra 900 using the Dynamac program.

Unless otherwise stated, all solvents and reagents were obtained commerically and used without further purification. Diethyl ether, heptane, and toluene were purified by distillation from alkali metal-benzophenone under nitrogen. Methylene chloride was distilled from P_2O_5. Deuterated solvents were purchased from Cambridge Isotope Laboratories. Benzene-d_6 was dried over benzophenone ketyl, and methylene chloride-d_2 was dried over calcium hydride. Deuterated Freon 21 ($CDFCl_2$) and Freon 22 (CDF_2Cl) were prepared according to the reported procedure[26] and purified by distillation at an ambient temperature of 4 °C. Absolute methanol was freeze−pump−thaw degassed prior to use. Distilled water and glacial acetic acid were purged with argon before use. Liquid phosphines were degassed and stored in vessels equipped with Teflon high-vacuum stopcocks. Solid phosphines were used without further purification, except tricyclohexylphosphine which was sublimed onto a water-cooled probe at 82 °C. $[(\eta\text{-}C_5Me_5)IrCl_2]_2$ was prepared according to the published procedure.[27]

Synthesis of Compounds. Compounds of the form $[(\eta\text{-}C_5H_5)Ir(L)H_3]BF_4$ were synthesized according to the published procedure[7] where L = P^iPr_3 (**13**), PCy_3 (**14**), PMe_3 (**15**), PPh_3 (**16**), and $AsPh_3$ (**17**).

(η-C_5Me_5)Ir(P^iPr_3)Cl_2 (1). A 250-mL Schlenk tube was charged with 200 mg (0.503 mmol Ir) of $[(\eta\text{-}C_5Me_5)IrCl_2]_2$, 88 mg (0.553 mmol) of P^iPr_3 and 20 mL of CH_2Cl_2. The resulting orange solution was stirred for 20 hours. The volume was reduced to 5 mL, and heptane was added to crystallize out **1** at 0 °C as a fine orange powder. Yield 269 mg, 96%. ^{1}H NMR at 298 K, 300 MHz ($CDCl_3$): δ 1.58 (s, 15 H, $C_5\mathit{Me}_5$), 2.75 (m, 3 H, PCHMe$_2$), 1.34 (dd, 18 H, PCHMe_2, $^3J_{PH}$ = 15.2 Hz, $^3J_{HH}$ = 6.7 Hz). Anal. Calcd for $C_{19}H_{36}PIrCl_2$: C, 40.85; H, 6.50. Found C, 40.94; H, 6.38. A similar procedure was used to prepare compounds **2**,[28] **3**,[29] and **4**.[27] Spectroscopic data were consistent with those reported in the literature.

(21) For definition of basicity used see: Tolman, C. A. *Chem. Rev.* **1977**, *77*, 313−348.

(22) Jarid, A.; Moreno, M.; Lledos, A.; Lluch, J. M.; Bertran, J. *J. Am. Chem. Soc.* **1995**, *117*, 1069−1075.

(23) Clot, E.; Leforestier, C.; Eisenstein, O.; Pelissier, M. *J. Am. Chem. Soc.* **1995**, *117*, 1797−1799.

(24) Limbach, H. H.; Scherer, G.; Maurer, M.; Chaudret, B. *Angew. Chem., Int.* **1992**, *31*, 1369−1372.

(25) Van Geet, A. L. *Anal. Chem.* **1970**, *42*, 679−680.

(26) Siegel, J. S.; Anet, F. A. L. *J. Org. Chem.* **1988**, *53*, 2629−2630.

(27) Kang, J. W.; Moseley, K.; Maitlis, P. M. *J. Am. Chem. Soc.* **1969**, *91*, 5970−5977.

(28) Freedman, D. A.; Mann, K. R. *Inorg. Chem.* **1991**, *30*, 836−840.

(29) Isobe, K.; Bailey, P. M.; Maitlis, P. M. *J. Chem. Soc., Dalton Trans.* **1981**, 2003−2008.

(η-C_5Me_5)Ir(P^iPr_3)H_2 (5). A 250-mL Schlenk flask was charged with 200 mg (0.36 mmol) of **1** and 15 mL of absolute MeOH. Zinc dust (0.5 g) and glacial acetic acid (1.3 mL) were added to this orange slurry. The resulting mixture was stirred for 20 hours giving a pale yellow solution. A saturated aqueous NaCl and NaOH solution (10 mL) was added. After 3 × 20 mL toluene extractions, the toluene extracts were combined, and the solvent was removed in vacuo. The resulting product **5** was a colorless oil, which crystallized upon extensive evacuation (48 h). Yield 158 mg, 90%. ^{1}H NMR at 298 K, 500 MHz (CD_2Cl_2): δ 2.1 (s, 15 H, C_5Me_5), 2.11 (m, 3 H, PC*H*Me_2), 1.15 (dd, 18 H, PCH*Me*$_2$, $^3J_{PH}$ = 15 Hz, $^3J_{HH}$ = 6.5 Hz), −18.7 (d, 2 H, IrH_2, $^2J_{PH}$ = 31.3 Hz). Anal. Calcd for $C_{19}H_{38}$PIr: C, 46.60; H, 7.82. Found C, 46.67; H, 7.61. Compounds **6**−**8** were prepared in a similar manner. For **6** ^{1}H NMR at 298 K, 300 MHz (C_6D_6): δ 2.16 (s, 15 H, C_5Me_5), 1.2−2 (m, 33 H, PC_6H_{11}), −18.75 (d, 2 H, IrH_2, $^2J_{PH}$ = 31.6 Hz). Anal. Calcd for $C_{28}H_{50}$PIr: C, 55.14; H, 8.26. Found C, 55.46; H, 8.03. For **7**[29] and **8**[30] spectroscopic data were consistent with those reported in the literature.

[(η-C_5Me_5)Ir(P^iPr_3)H_3][BF_4] (9). A 50-mL Schlenk tube was charged with 100 mg (0.20 mmol) of **5** and 10 mL of CH_2Cl_2. Next 50 μL of HBF_4·Et_2O was added dropwise with stirring. After the solution stirred for 20 min, the volume was reduced to approximately 2 mL, and 10 mL of Et_2O was added. After immediate precipitation of the white solid **9** occurred, it was washed with 3 × 5 mL cold Et_2O. The remaining solvent was removed in vacuo: yield 93 mg, 95%. The cations **10**−**12** were prepared by the same method. See Table 1 for analytical and room temperature ^{1}H NMR data for **9**−**12**. ^{1}H NMR of hydride region only, at 163 K, 500 MHz ($CDCl_2F$): For **9**, δ −13.78 (dt, 1 H, Ir$H_A(H_B)_2$, $^2J_{PH}$ = ±6.0 Hz, $^2J_{AB}$ = 21.0 Hz), −13.97 (dd, 2 H, Ir$H_A(H_B)_2$, $^2J_{PH}$ = ∓19.7 Hz, $^2J_{AB}$ = 21.0 Hz). For **10**, δ −13.91 (dd, 2 H, Ir$(H_A)_2H_B$, $^2J_{PH}$ = ∓19.8 Hz, $^2J_{AB}$ = 20.1 Hz), −14.04 (dt, 1 H, Ir$(H_A)_2H_B$, $^2J_{PH}$ = ±6.0 Hz, $^2J_{AB}$ = 20.1 Hz). For **12**,[32] δ −12.13 (m, 1 H, Ir$H_A(H_B)_2$, $^2J_{PH}$ = ±12.2 Hz, $^2J_{AB}$ = 51.2 Hz), −13.00 (m, 2 H, Ir$H_A(H_B)_2$, $^2J_{PH}$ = ∓19.5 Hz, $^2J_{AB}$ = 51.2 Hz). For **11** the low temperature spectroscopic data were consistent with those reported in the literature.[31]

Deuterium Incorporation. Compounds **9**−**17**, in 10.0 mg quantities, were placed in NMR tubes equipped with Kontes high vacuum stopcocks. Approximately 1.2 mL of $CDCl_2F$ was vacuum transferred into each tube. The samples were freeze−pump−thaw degassed three times each and charged with 810 Torr deuterium gas (D_2). The samples exchanged with D_2 at ambient temperature for a specified amount of time, depending on the particular experiment, with no agitation. They were then degassed an additional three times, and the tubes were flame-sealed under vacuum.

Tritium Incorporation. A tritium incorporation apparatus was developed, consisting of a stainless steel vacuum manifold with in-line diffusion and vacuum pumps. The apparatus is equipped with both a pressure and a vacuum gauge. One end of the manifold has an external Nupro sealed-bellows valve allowing for input of H_2, D_2, or an inert gas. The opposite end of the vacuum manifold consists of a permanent Cajon connector for attachment of an NMR tube. Attached directly to the manifold by a Nupro valve is a hollow, stainless steel cylinder filled with activated coconut charcoal. The charcoal was initially activated by heating to 580 °C, under vacuum for 12 h. Tritium gas (T_2) was adsorbed on the activated coconut charcoal at 77 K and stored at ambient temperature.

Compounds **9**−**17**, in 1.0 mg quantities, were placed in NMR tubes equipped with Rotoflo, low volume, high vacuum stopcocks. Approximately 1.2 mL of CD_2Cl_2 was vacuum transferred into each tube. The samples were freeze−pump−thaw degassed three times each and attached to the tritium incorporation apparatus. The T_2 was released, at ambient temperature, into the head space of an NMR tube over a frozen solution of each of **9**−**17**. The average pressure of T_2 over each sample was 200 Torr. The thawed samples exchanged with T_2 for 6−8 hours, on average, depending on the rate of incorporation which was determined through deuterium exchange studies. The samples were then thoroughly degassed, with the remaining gas readsorbed onto the charcoal at 77 K for storage and reuse. The NMR tubes were flame-sealed under vacuum. Incorporation of T appeared to be expedited by self-radiolysis within the sample and occurred approximately three times faster than the exchange of D, from D_2, under similar pressures and conditions. Total sample activity did not exceed 10 mCi/sample by assay.

Table 1. ^{1}H NMR Data and Analyses for **9**−**12**[a]

	L	protons	δ,[b] ppm	coupling[c]	calcd C	calcd H	found C	found H
9	P^iPr_3	C_5Me_5	2.3 (s)		39.52	6.81	39.74	6.91
		$PCHMe_2$	2.11 (m)					
		$PCCH_3$	1.17 (dd)	$^3J_{HH}$ = 6.45				
				$^3J_{PH}$ = 15.7				
		IrH_3	−13.9 (d)	$^2J_{PH}$ = 11.1				
10	PCy_3	C_5Me_5	2.28 (s)		48.20	7.37	48.31	7.35
		PC_6H_{11}	1.2−2 (m)					
		IrH_3	−14.05 (d)	$^2J_{PH}$ = 11.2				
11	PMe_3[d]	C_5Me_5	2.3 (d)	$^3J_{PH}$ = 1.6				
		PCH_3	1.83 (d)	$^2J_{PH}$ = 11.8				
		IrH_3	−13.5 (d)	$^2J_{PH}$ = 10.1				
12	PPh_3[e]	C_5Me_5	2.04 (d)	$^3J_{PH}$ = 1.85				
		PC_6H_5	7.3−7.5 (m)					
		IrH_3	−12.7 (d)	$^2J_{PH}$ = 8.9				

[a] Spectra of the cationic trihydrides [(η-C_5Me_5)Ir(L)H_3]BF_4 **9**−**12** were obtained in $CDCl_2F$ at ambient temperature, 500 MHz. [b] Chemical shifts are referenced to TMS. [c] Coupling constants are reported in Hz. [d] **11** has been previously reported, ref 31. [e] **12** has been previously reported, ref 32.

Results

Synthesis. The dichloride compounds, (η-C_5Me_5)Ir(L)Cl_2, L = $PiPr_3$ (**1**), PCy_3 (**2**), PMe_3 (**3**), and PPh_3 (**4**), were prepared by a slight variation of the method of Maitlis and co-workers.[27] Compounds **2**,[28] **3**,[29] and **4**[27] are known compounds, but **1** has not been previously reported. Reduction of **1**−**4** gives the corresponding dihydride complexes, **5**−**8**, following the method of Moss and Graham.[33] The dihydrides, **5**−**8**, are mildly air sensitive, colorless solids. Compounds **7**[29] and **8**[28,32] have been prepared before by alternate methods, whereas **5** and **6** have not been previously reported. Protonation (HBF_4·Et_2O) of the neutral dihydrides affords the salts [(η-C_5Me_5)Ir(L)H_3]BF_4, **9**−**12**, in fair yields. These complexes are colorless and very air sensitive both in solution and as solids. Of these compounds, **11**[31] and **12**[32] have been reported previously. Analytical and ^{1}H NMR data for **9**−**12** are given in Table 1, while appropriate data for **1**, **5**, and **6** can be found in the Experimental Section above.

Proton NMR Observations. The hydride ligands in **9**−**17** undergo a thermally activated rearrangement, rendering them equivalent on the NMR time scale at temperatures above 220 K. Thus all three hydride ligands give rise to one ^{1}H NMR signal at an averaged chemical shift around −13 ppm. At low temperature the signal decoalesces into two resonances, often split into complex patterns consistent with either an AB_2X or an A_2BX spin system. Chemical shifts and coupling constants for **9**−**17** were determined by computer simulation of these low temperature spectra. This data are reported for **9**−**12** in the Experimental Section above. Line shape analysis of the ^{1}H NMR spectra for **9**−**17** at various temperatures yielded rate data, which was incorporated into an Eyring plot for each compound. The corresponding enthalpies, entropies, and free energies of activation for the rearrangement of the hydrides within **9**−**17** were derived. The activation barriers for rearrangement observed for **9**−**12** are higher than those for **13**−**17**. The calculated activation parameters for **9**−**17** are reported in Table 2.

(30) Janowicz, A. H.; Bergman, R. G. *J. Am. Chem. Soc.* **1983**, *105*, 3929−3929.

(31) Gilbert, T. M.; Bergman, R. G. *J. Am. Chem. Soc.* **1985**, *107*, 3502−3507.

Table 2. Activation Parameters for the Thermally Activated Rearrangement of the Hydride Ligands for **9**−**17**

	L	$\Delta G^{\ddagger} \pm 0.6$ kcal/mol[a]	$\Delta H^{\ddagger} \pm 0.4$ kcal/mol	$\Delta S^{\ddagger} \pm 1.1$ eu
9	P^iPr_3	11.2	11.8	1.1
10	PCy_3	11.4	12.0	1.0
11	PMe_3[b]	10.6	11.0	0.7
12	PPh_3	10.1	10.4	0.5
13	P^iPr_3	9.6	10.1	0.8
14	PCy_3	9.9	10.3	0.6
15	PMe_3	9.4	9.6	0.4
16	PPh_3	9.3	9.5	0.3
17	$AsPh_3$	8.7	9.2	0.9

[a] $\Delta G^{\ddagger}$ calculated at 298 K. [b] Activation parameters for **11** have been reported previously, ref 31.

Low temperature ^{1}H NMR spectra were obtained from 220 K down to 125 K for **9**−**17**. At all temperatures the resonances for the hydride sites A and B were distinguishable. The magnitude of the observed H_A-H_B coupling constant (J_{AB}) was very sensitive to temperature, increasing as temperature increased. Values for J_{AB} have not previously been available over such a large range of temperatures. The values for J_{AB} at each temperature vary widely for **9**−**17** and appear to be very sensitive to the basicity of the coligands. For **9** and **10** J_{AB} changes less than 1 Hz from 170 to 125 K. Variable-temperature ^{1}H NMR data for **9**−**17** is tabulated in Table 3.

NMR Analyses of Partially Deuterated Trihydride Cations. Complexes **9**−**17** incorporate D into the hydride sites readily upon exposure in solution to D_2. ^{1}H NMR spectra were obtained over a 100 K range of temperatures for partially deuterated samples of **9**−**17**. The observed isotopomers will be represented by the notation below in which Ir is the organometallic fragment, $[(\eta\text{-}C_5R_5)Ir(L)]BF_4$ (R = H, Me). Resonances were apparent for the three detectable isotopomers $Ir(H)_3$, $Ir(H)_2D$, and $IrH(D)_2$. Below 220 K, resonances for the different hydride sites A and B are distinguishable, and isotope effects on the chemical shifts corresponding to each site were observed. These upfield isotope shifts are temperature independent and large enough to allow observation of separate resonances for each isotopomer, as exemplified for **9** in pictorial format, in Figure 1. The $Ir(H)_2D$ isotopomer has two positional isomers, with D in site A or in one of the B sites, which we will designate as $Ir(H_B)_2D_A$ and $IrH_BH_AD_B$, respectively. The former isomer exhibits one resonance in the hydride region of a ^{1}H NMR spectrum, while the latter gives an eight-line pattern typical of an ABX spin system. Similar considerations apply to the $IrH(D)_2$ isotopomer where each of the two possible positional isomers gives rise to one resonance in the hydride region of a ^{1}H NMR spectrum.

Within the ^{1}H NMR spectra for partially deuterated **9**−**17** there are two observable H_A-H_B coupling constants, J_{AB} for $Ir(H)_3$ and J_{AB} for $IrH_BH_AD_B$. The J_{AB} values, derived by computer simulation of the ^{1}H NMR spectra, for $IrH_BH_AD_B$ are 4−8% larger than the J_{AB} values derived for the $Ir(H)_3$ species, for **13**−**17**. However for **9**−**12**, there appears to be no difference in these two coupling constants. Small unresolved H−D couplings caused the ^{1}H NMR resonances of the hydrides in the deuterated isotopomers to be slightly broader than those corresponding to $Ir(H)_3$ for **9**−**17**. Results of the ^{1}H NMR studies of the partially deuterated cations are given in Table 4.

NMR Analyses of Partially Tritiated Trihydride Cations. Complexes **9**−**17** were exposed to T_2 to form mixtures of the isotopomers: $Ir(H)_3$, $Ir(H)_2T$, $IrH(T)_2$, and $Ir(T)_3$. Both ^{3}H and ^{1}H NMR spectra were obtained for partially tritiated **9**−**17** at various temperatures. Temperature independent, upfield isotope effects on the chemical shifts upon tritium substitution were observed. These tritium isotope shifts follow the same pattern as, but are slightly larger than, the deuterium isotope shifts shown in Figure 1. The tritium isotope shifts were identical for hydride resonances in the ^{1}H NMR spectra and tritide resonances in the ^{3}H NMR spectra.

The isotopomers $Ir(H)_2T$ and $IrH(T)_2$ each have two positional isomers. Thus resonances for these tritiated species $IrH_BH_AT_B$, $Ir(H_B)_2T_A$, $IrH_A(T_B)_2$, $IrH_BT_AT_B$, and $IrT_A(T_B)_2$ are all detectable in the low temperature ^{3}H NMR spectra of **9**−**17**. A representative ^{3}H NMR spectrum, hydride region only, is shown in Figure 2 for **14**. In contrast to the ^{1}H NMR spectra, which often exhibit second order line patterns for the hydride resonances, the ^{3}H NMR spectra are first order. Observed in the ^{3}H NMR spectra for **9**−**17** are temperature independent H−T coupling constants (J_{HT}). The values for J_{HT} are smaller than the values for J_{AB} observed in the ^{1}H NMR spectra, while the A−B chemical shift difference is the same, giving rise to first order line patterns. The temperature independent values of J_{HT} were used to ascertain the values for the magnetic H_A-H_B coupling constant (J_{mag}) for **9**−**17**, based on the ratio of magnetogyric ratios for the isotopes:[35] $\gamma_T/\gamma_H = 1.07$. Results of the ^{3}H NMR studies of the partially tritiated cations are given in Table 5. For **9**, **13**, **14**, **16**, and **17** J_{TT} was also observed ranging from 19.3 to 31.1 Hz and temperature independent.

A representative ^{1}H NMR spectrum of the hydrides for partially tritiated **14** is also shown in Figure 2. The isotopomers $Ir(H)_3$ and $Ir(H)_2T$ both give rise to resonances in this spectrum. The observed J_{AB} for the $Ir(H)_3$ isotopomer is 85 Hz, while J_{AB} for $IrH_BH_AT_B$ is 91 Hz. ^{1}H NMR spectra for compounds **13** and **16** also allowed this comparison, and the J_{AB} for $IrH_BH_AT_B$ was larger at all temperatures observed.

Line shape analysis of the hydride region of ^{1}H and ^{3}H NMR spectra for partially tritiated **9**−**17** was performed. The line width of the ^{1}H NMR resonances seemed unaffected by the substitution of tritons, indicating the absence of significant kinetic isotope effects on the thermally activated rearrangement process. Also no differential line broadening was observed in comparison of the resonances for the hydrides and tritides in the $Ir(H)_3$ and $Ir(T)_3$ isotopomers.

Discussion

Synthesis. Previously the conversion of the metal halides $(\eta\text{-}C_5Me_5)Ir(L)Cl_2$ to hydrides has been achieved with a variety of borohydride or aluminum hydride reagents.[29,28] We have found that reduction by a modification of the zinc/acetic acid/methanol procedure of Moss and Graham[33] is more convenient and gives slightly better yields. The resulting products are crystalline and require little purification.

Tritium Incorporation. The most common method for tritium incorporation into compounds is by exposing the compound to HTO.[34] Since many transition-metal hydrides, including **9**−**17**, are air and moisture sensitive, this was not a suitable method for our purposes. An incorporation method was sought to allow for safe, efficient processing of many samples while minimizing unwanted side reactions. The cations **9**−**17** exchange readily with T_2 at ambient temperatures, in solution. A tritium incorporation apparatus was developed for storage and handling of T_2, consisting of a stainless steel vacuum manifold with in-line diffusion and vacuum pumps. One end of the vacuum manifold consists of a permanent Cajon connector for attachment of an NMR tube. Attached directly to the

(32) Pedersen, A.; Tilset, M. *Organometallics* **1993**, *12*, 3064−3068.
(33) Moss, J. R.; Graham, W. A. G. *Inorg. Chem.* **1977**, *16*, 75−79.
(34) Evans, E. A. *Tritium and Its Compounds*; 2nd ed.; Wiley: New York, 1974; pp 272−290.

Table 3. Temperature and Ligand Dependence of J_{AB}[a–c]

	L	125 K	135 K	144 K	154 K	163 K	173 K	182 K	191 K	201 K
9	P^iPr_3	20.0	20.0	20.0	20.3	21.0	21.9	22.3	22.8	23.9
10	PCy_3	20.1	20.1	20.1	20.1	20.1	20.1	20.3	20.9	23.4
11	PMe_3	30.5	31.2	32.3	33.6	35.8	38.3	42.4	48.8	59.0
12	PPh_3	36.8	40.1	43.0	46.5	51.2	56.0	66.8	79.3	99
13	P^iPr_3	47.4	48.6	52.7	54.6	57.4	66.2	73.4	82	94
14	PCy_3	43.5	48.3	50.2	54.0	57.9	63.8	70.4	80.1	95
15	PMe_3	71.7	75.8	80.7	84	93	106	123	140	168
16	PPh_3	160	174	188	216	247	292	348	422	533
17	$AsPh_3$	218	237	262	304	353	428	524	642	828

[a] All spectra were obtained in $CDCl_2F$, 500 MHz. [b] Coupling constants are reported in Hz. [c] There are some discrepancies between the previous and current NMR data for **13**−**17**, which we believe are due to a systematic temperature calibration error.

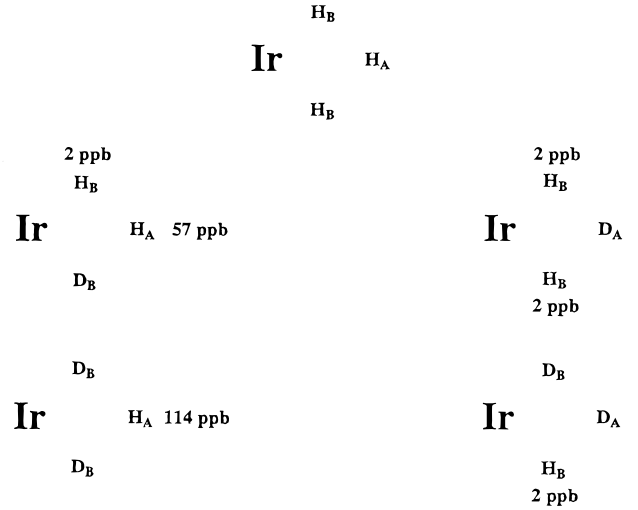

Figure 1. Isotope effects on the chemical shifts of the various isotopomers of partially deuterated **9**. Shifts are reported in parts per billion (ppb) and are upfield from the chemical shift of the pure protio species.

Table 4. ^1H NMR Data for Deuterium Substitution Studies (Hydride Region) of **9**−**17**[a]

	L	J_{AB}[b] for $Ir(H)_3$	J_{AB}[b] for $Ir(H)_2D$	site A ave $\Delta\delta/D$[c]	site B ave $\Delta\delta/D$[c]
9	P^iPr_3	22.3	22.3	57	2
10	PCy_3	20.3	20.3	60	4
11	PMe_3	42.4	42.4	70	6
12	PPh_3	66.8	66.8	66	4
13	P^iPr_3	73.4	76.3	66	32
14	PCy_3	70.4	73.2	70	35
15	PMe_3	123	129	72	36
16	PPh_3	347	368	74	38
17	$AsPh_3$	524	560	76	46

[a] All spectra were obtained in $CDCl_2F$, at 182 K, 500 MHz. [b] Coupling constants are reported in Hz. [c] Chemical shift differences are reported in ppb.

manifold by a sealed bellows valve is a hollow, stainless steel cylinder filled with activated coconut charcoal. T_2 was adsorbed on the charcoal at 77 K and stored at ambient temperature. Further details are described in the Experimental Section above. By taking advantage of its reversible adsorption on activated charcoal, the T_2 can be controlled and reused numerous times. The use of T_2 at pressures below 760 Torr increases the safety of the incorporation process.

By substituting T into the hydride sites of **9**−**17** we have introduced another useful NMR handle into these metal hydride systems. ^3H NMR spectra were obtained on a 500 MHz spectrometer with a ^3H probe at 533 MHz. ^3H NMR affords better spectral dispersion and is more sensitive than ^1H NMR spectroscopy. The chemical shifts of detected tritons are virtually the same as those of the corresponding protons.

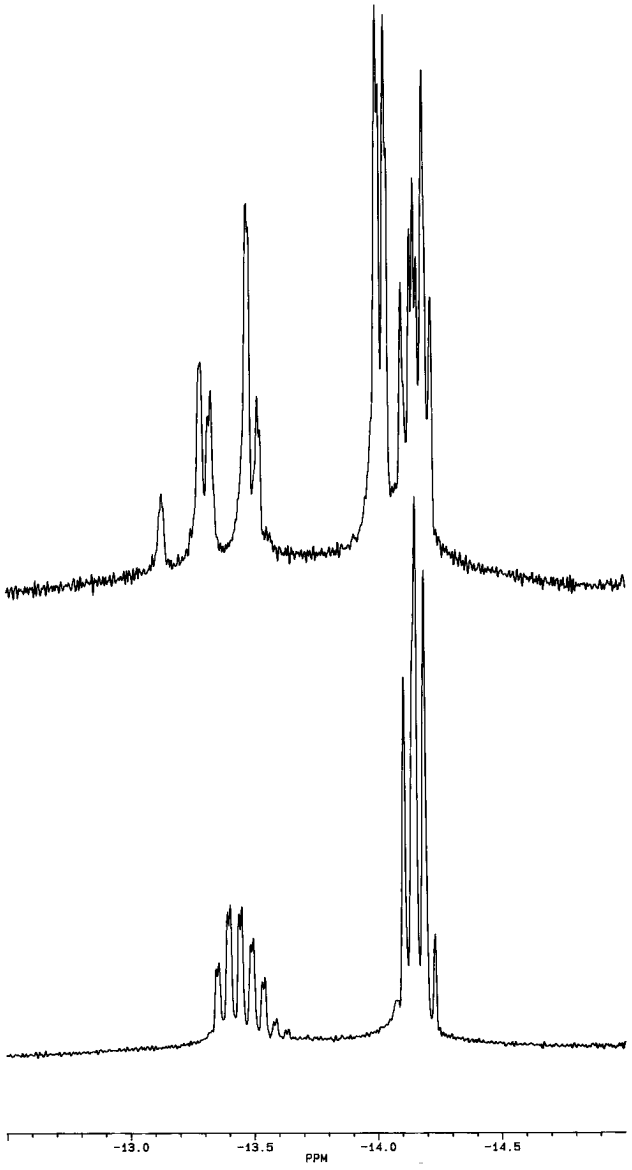

Figure 2. Experimental ^1H NMR (top) and ^3H NMR (bottom) spectra of partially tritiated **14**, hydride region only, (CD_2Cl_2, 195 K, 500 MHz and 533 MHz respectively). Coupling constants are $J_{AB} = 85$ Hz for $Ir(H)_3$, $J_{AB} = 91$ Hz for $IrH_BH_AT_B$, $J_{HT} = 24.7$, $J_{PH_A} = \pm 6$ Hz, $J_{PH_B} = \mp 17$ Hz (top); $J_{TT} = 26.4$ Hz, $J_{HT} = 24.7$ Hz, $J_{PT_A} = \pm 6.4$ Hz, $J_{PT_B} = \mp 18$ Hz (bottom).

Coupling constants for interaction of T with other spin active nuclei can be retlated to the corresponding H coupling constants by the ratio[35] $\gamma_T/\gamma_H = 1.07$. This method is frequently used in deriving such information for protons in organic molecules.[36] ^3H NMR is particularly useful because J_{HT} is 1.07 times larger

(35) Fuller, G. H. *J. Phys. Chem., Ref. Data* **1976**, *5*, 835.

Table 5. ^{3}H NMR Data for Tritium Substitution Studies (Hydride Region) for **9**−**17**[a]

	L	J_{HT}	calcd J_{mag}[b,c] for H_A-H_B	site A ave $\Delta\delta/T$[d]	site B ave $\Delta\delta/T$[d]
9	P^iPr_3	19.1	17.9	113	3.8
10	PCy_3	20.7	19.5	107	3.8
11	PMe_3	22.7	21.3	113	3.8
12	PPh_3	24.8	23.2	116	3.8
13	P^iPr_3	24.3	22.8	90	5.6
14	PCy_3	24.7	23.2	86	5.6
15	PMe_3	27.3	25.6	96	5.6
16	PPh_3	29.4	27.6	101	5.6
17	$AsPh_3$	28.7	26.9	104	5.6

[a] All spectra were obtained in CD_2Cl_2, at 200 K, 533 MHz. [b] $J_{HH} = J_{HT}/1.06667$ based on the magnetogyric ratios of H and T. [c] Coupling constants are reported in Hz. [d] Chemical shift differences are reported in ppb.

than J_{HH} and thus easily observed. However J_{HD} is 6.54 times smaller than J_{HH} and is often difficult to detect. The values of J_{HT} observed for **9**−**17** were in fact much smaller than the corresponding values of J_{AB} and they were temperature independent. This was expected because J_{AB} arises from a combination of a magnetic coupling and an exchange coupling interaction. Quantum mechanical exchange coupling should be quenched by T substitution in **9**−**17**.[7,8] Thus J_{HT} is presumably magnetic in origin, due principally to the Fermi contact mechanism. We were then able to derive the values of J_{mag} for **9**−**17** which have been reported for very few metal hydride complexes.

Thermally Activated Hydride Rearrangements. In addition to quantum mechanical exchange coupling, there is also a facile, thermally activated rearrangement process occurring in **9**−**17**. The stiffness of the Ir−H bonds and the corresponding vibrational frequencies would presumably affect this process in some manner, as it affects the quantum mechanical exchange coupling process. Thus a comparison of the activation barriers for the thermally activated rearrangement with the magnitude of the exchange coupling could be insightful. Qualitatively a correlation is apparent within each system **9**−**12** and **13**−**17**, where the magnitude of the exchange coupling increases as the barrier to the thermally activated rearrangement decreases. As seen in Table 2 the activation barriers for rearrangement within **9**−**12** are higher than those for **13**−**17**. This was predicted since the same factors causing less quantum mechanical exchange coupling interaction in **9**−**12** should have some influence on the difficulty of the thermal rearrangement as well.

Line shape analysis of ^{1}H NMR spectra for sample containing $Ir(H)_3$, $Ir(H)_2D$, and $IrH(D)_2$ yielded no apparent isotope effect on the rate of the thermally activated rearrangement. Slight differences in signal line widths, between the deuterated isotopomers and the perprotio species, were determined to be unresolvable splittings due to H−D couplings. From computer simulation of the hydride resonances in these ^{1}H NMR spectra the values for J_{HD} were derived to be 2−4 Hz, depending on the complex. These values for J_{HD} agree well with the experimental values obtained for J_{HT}, which should be seven times larger than those for J_{HD}. Line shape analysis of spectra generated by both ^{1}H and ^{3}H NMR, of the tritium isotopomers as compared to the perprotio species, yielded no evidence of differential line broadening.

There seems to be no appreciable kinetic isotope effect, k_H/k_D or k_H/k_T, on the thermally activated hydride rearrangement process. Interpretation of this result is somewhat ambiguous in that known isotope effects on dihydrogen reductive elimination/oxidative addition are not very large. Thus it seems that formation and rotation of a dihydrogen ligand cannot be ruled out as a mechanism for hydride rearrangement in **9**−**17**.

Elucidation of J_{AB}. A brief introduction to quantum mechanical exchange coupling as it relates to **9**−**17** is appropriate here. For two hydride ligands bonded to a metal center, if each H atom is strongly localized in its respective potential energy well, then the vibrational motion of each can be treated independently. However, if the H atoms are close enough to each other, with appropriate harmonic oscillator frequencies, then their orbital wave functions may overlap.[8] The vibrational motion of the two H atoms can no longer be treated independently; instead the two-particle system must be considered as a whole. This finite overlap gives rise to both a symmetric and an antisymmetric combination of the two single-particle wave functions,[8] which differ in energy by an amount $2J_{ex}$. The term J_{ex} here represents the quantum mechanical exchange coupling between two adjacent hydrides in metal hydride systems. It has been generally accepted that quantum mechanical exchange coupling is manifest in the ^{1}H NMR spectra of various metal hydride complexes according to the following expression[8]

$$J_{AB} = J_{mag} - 2J_{ex} \quad (1)$$

where J_{mag} is the portion of J_{AB} due to the Fermi contact interaction. The sign of J_{mag} is not predicted by eq 1 and may vary from compound to compound. However according to the proposed model for quantum mechanical exchange coupling, J_{ex} is inherently negative. As mentioned above, we have now been able to derive J_{mag} from the observed values of J_{HT} for **9**−**17**.

There are very few values for H−H coupling constants for transition-metal hydride complexes reported in the literature. Typically these complexes are very dynamic, with the hydride ligands rearranging rapidly at ambient temperature. Thus it is necessary to obtain low temperature ^{1}H NMR spectra for the complexes in order to detect H−H coupling. Even then, the barriers to thermal rearrangement for some complexes are low enough that the ^{1}H NMR resonances for the hydrides do not decoalesce at accessible temperatures. Those values for H−H couplings which have been reported for transition-metal hydride systems vary from 2−18 Hz.[37] It may be their cationic nature which leads to values of 18−28 Hz for **9**−**17**. However, since the existing database for such information is small, no firm conclusions can be made.

The determined values of J_{mag} for **9**−**17** were used to calculate the values of the corresponding J_{ex} at each temperature according to eq 1. The results are shown in Table 6. The quantum mechanical exchange coupling model describes J_{ex} as

(36) Evans, E. A.; Warrell, D. C.; Elvidge, J. A.; Jones, J. R. *Handbook of Tritium Nuclear Magnetic Resonance Spectroscopy and Applications*; Wiley: New York, 1985.

(37) Some representative two-bond, H−H couplings reported for various transition-metal hydride complexes are referenced here: J_{HH} = 2.2 Hz and 5.5 Hz for the fac isomer of $[H_3Ir(NH(SiMe_2CH_2PPh_2)_2)]$ and J_{HH} = 5.0 Hz for the mer isomer; J_{HH} = 5.1 Hz for the mer-cis isomer of $[H_2IrN(SiMe_2CH_2PPh_2)_2(PMe_3)]$ and J_{HH} = 4.0 Hz for the fac-cis isomer; J_{HH} = 4.4 Hz for the mer-cis isomer of $[H_2IrN(SiMe_2CH_2PPh_2)_2(CO)]$. [Fryzuk, M. D.; MacNeil, P. A. *Organometallics* **1983**, *2*, 682−684]. J_{HH} = 4 Hz for $(C_5Me_5)_2NbH_3$. [Bell, R. A.; Cohen, S. A.; Doherty, N. M.; Threlkel, R. S.; Bercaw, J. E. *Organometallics* **1985**, *5*, 972−975.] J_{HH} = 5.5 Hz for cis,trans-$[IrH_2$(endo-5-norbornen-2-ol)-$(PPh_3)_2]BF_4$. [Crabtree, R. H.; Davis, M. W. *Organometallics* **1983**, *2*, 681−682.] J_{HH} = 5.6 Hz for $(C_5Me_5)Ir(SiMe_3)H_3$; J_{HH} = 6.5 Hz for $(C_5Me_5)Ir(SnMe_3)H_3$; J_{HH} = 8.1 Hz for $(C_5Me_5)Ir(SnPh_3)H_3$. [Gilbert, T. M.; Hollander, F. J.; Bergman, R. G. *J. Am. Chem. Soc.* **1985**, *107*, 3508−3516.] J_{HH} = 8.9 Hz for $(C_5Me_5)Os(CO)H_3$. [Hoyano, J. K.; Graham, W. A. G. *J. Am. Chem. Soc.* **1982**, *104*, 3722−3723.] J_{HH} = −14 Hz for $H_2Ru[P(OMe)_3]_4$. [Meakin, P.; Muetterties, E. L.; Jesson, J. P. *J. Am. Chem. Soc.* **1973**, *95*, 75−90.] J_{HH} = 18.2 Hz for *trans*-FeH_2-(meso-tetraphos-1). [Bautista, M. T.; Earl, K. A.; Maltby, P. A.; Morris, R. H. *J. Am. Chem. Soc.* **1988**, *110*, 4056−4057.]

Table 6. Temperature and Ligand Dependence of J_{ex}[a,b]

	L	125 K	135 K	144 K	154 K	163 K	173 K	182 K	191 K	201 K
9	P^iPr_3	−1.1	−1.1	−1.1	−1.2	−1.6	−2.0	−2.2	−2.5	−3.0
10	PCy_3	−0.3	−0.3	−0.3	−0.3	−0.3	−0.3	−0.4	−0.7	−2.0
11	PMe_3	−4.6	−4.7	−5.2	−5.9	−7.0	−8.2	−10.3	−13.5	−18.9
12	PPh_3	−6.8	−8.5	−9.9	−11.7	−14.0	−16.4	−21.8	−28.1	−38
13	P^iPr_3	−12.6	−14.7	−15.6	−17.0	−21.4	−25.0	−29.3	−35	−44
14	PCy_3	−10.2	−12.6	−13.5	−15.4	−17.4	−20.3	−23.6	−28.5	−36
15	PMe_3	−23.2	−25.2	−27.7	−29	−34	−41	−49	−57	−71
16	PPh_3	−67	−73	−80	−94	−110	−132	−160	−197	−253
17	$AsPh_3$	−95	−105	−118	−139	−163	−201	−249	−308	−401

[a] All results were calculated according to eq 1. [b] Coupling constants are reported in Hz.

being inherently negative.[8] Taking this into consideration, we attempted to computer fit the two J_{ex} versus temperature data sets arising from having J_{mag} be both positive and negative. There was no obtainable fit for the data resulting from J_{mag} being negative which would be physically reasonable. It would appear that the sign of J_{mag} is opposite to that of J_{ex} for **9**−**17**, whereas for $(\eta\text{-}C_5H_5)_2NbH_3$ which was reported previously,[10] the sign of J_{mag} appears to be the same as that of J_{ex}. In support of this, J_{AB} was not observed to decrease to a value of 0 Hz and then increase again with decreasing temperature for **9**−**17**. However such behavior was observed for $(\eta\text{-}C_5H_5)_2NbH_3$, indicating that J_{mag} and J_{ex} canceled each other out at some temperature.[10] This would arise from J_{mag} and J_{ex} having the same sign when combined as in eq 1. There is some precedence for variation of the sign of two-bond, H−H coupling constants. In fact, the geminal H−H coupling constants in organic compounds vary from −23 to +42 Hz depending on ligand substitution at the α-carbon.[38] Thus it is reasonable that the cationic iridium trihydrides have positive values of J_{mag} and the neutral niobium trihydride has a negative value of J_{mag}.

Quantum Mechanical Exchange Coupling. In our initial reports for **13**−**17**, we had collected NMR data over a 20−30 K range. The use of an NMR probe specially designed for spectroscopy at low temperatures has now allowed collection of data over a 100 K range, including lower temperatures than previously accessible. With these larger data sets it became apparent that the previously reported three-dimensional model for quantum mechanical exchange coupling does not correctly describe the temperature dependence of J_{ex} for **9**−**17**. While the three-dimensional model appeared to fit the previous data,[8] it could not fit the new lower temperature data now available. However a *two-dimensional* description of quantum mechanical exchange coupling does accurately describe the current J_{ex} versus temperature data. The three-dimensional model originally reported[8] was based on work done for the $^3He/^4He$ system in which atomic motion is governed by the solid lattice. In solid helium each He atom has only He neighbors surrounding it; therefore atomic motion and quantum mechanical exchange coupling are equally probable in all three dimensions.

In contrast to solid helium, in the metal trihydride complexes studied here neutron diffraction data indicate that the potential describing bond stretches is much stiffer than the potential describing motions perpendicular to bond stretches.[7] The hydrogen atoms are in effect confined by this potential to move on a two-dimensional surface. In this case it is appropriate to apply the Landesman model of exchange in two rather than three dimensions. An expression for the ground state exchange coupling in two dimensions has been derived following the calculation of Landesman in three dimensions. The hydrides are modeled as hard sphere fermions bound in a symmetric two dimensional double-well potential. Heitler−London wave functions formed from linear combinations of localized Gaussian wave functions correlated by a step correlation function appropriate for hard spheres approximately describe the lowest lying excited states of the hydrogen atoms in the double well potential. These wave functions are used in the two-dimensional analog of Landesman's surface integral expression for the calculation of ground state exchange.

Temperature dependence is included in the model by assuming that the potential binding the hydrides is temperature independent and that the observed temperature dependence of the exchange interaction is a consequence of the thermal population of excited vibrational states of the hydrides. It is further assumed that the exchange process can be calculated separately in each vibrational state and therefore that the exchange interaction at temperature T can be written as the sum over all vibrational states of the exchange interaction in each state. This sum is in turn proportional to the sum over ground and excited vibrational states of the overlap of the localized wave functions weighted by the appropriate Boltzmann factor. This total overlap function is approximated by giving the ground state wave function a temperature dependent width equal to the root mean square displacement of a two-dimensional harmonic oscillator at temperature T. A more detailed discussion of this method and justification of the approximations involved can be found in our previous paper.[8] The derivation of the expression for ground state exchange of two hard sphere fermions in two dimensions is presented in a separate paper.[39] The result of the derivation of two-dimensional exchange as outlined above gives J_{ex} in units of Hertz as

$$J_{ex} = \left(\frac{-\hbar a}{2m\pi^2\lambda\delta^2}\right)\exp\left\{\frac{-(a^2+\lambda^2)}{2\delta^2}\right\} \qquad (2)$$

and

$$\delta^2 = \left[\frac{h}{4\pi^2 m\nu}\right]\coth\left[\frac{h\nu}{2kT}\right]$$

where δ^2 is the mean square displacement of an ensemble of two dimensional harmonic oscillators at temperature T, a is the internuclear distance, m is particle mass, and λ is the hard sphere radius of the particles. The expression for δ^2 describes the ensemble-mean delocalization of the hydrides. Increasing temperature results in thermal population of excited vibrational states of the hydrides leading to a larger observed exchange coupling. A purely Gaussian description of quantum exchange has the hydrides passing through each other at the high energy limit of the interaction. The inclusion of λ in eq 2 lowers the probability that the exchange interaction will occur when the hydrides are too close to each other. Essentially repulsive terms in the exchange interaction limit the amount of mixing of the spatial wave functions which will occur. By fitting the J_{ex}

(38) Günther, H. *NMR Spectroscopy*; Wiley: New York, 1980; pp 100−106.

(39) Close, J. personal communication.

Table 7. Results from Fitting J_{ex} versus Temperature Data to the Two-Dimensional Quantum Mechanical Exchange Coupling Model, Eq 2, for **9**−**17**

	L	λ, Å	a, Å	ν, cm^{-1}
9	P^iPr_3	1.1	1.70	494
10	PCy_3	1.1	1.70	497
11	PMe_3	1.1	1.73	458
12	PPh_3	1.1	1.72	452
13	P^iPr_3	0.9	1.70	502
14	PCy_3	0.9	1.70	503
15	PMe_3[a]	0.9	1.69	499
16	PPh_3	0.9	1.72	463
17	$AsPh_3$	0.9	1.74	456

[a] For **15**, a has been reported previously from neutron diffraction data to be 1.686 Å.

versus temperature data to eq 2, it was hoped that unique combinations of a, λ, and ν, which were physically reasonable, could be determined for **9**−**17**.

Computer fitting of the experimental data in this manner gives an apparent λ of 1.1 Å for **9**−**12** and 0.9 Å for **13**−**17**. In molecular mechanics calculations for organic species, λ is assigned a value of 1.37 Å for H attached to aliphatic carbons and $\lambda = 1$ Å for H attached to N, O, or S.[40] These values for λ are based on experimental gas viscosity data for small molecules. Nonbonding, attractive interactions between the molecules are replaced by repulsive interactions when the molecules reach an intermolecular distance of closest approach.[41] A larger value for λ corresponds to greater electron density on the hydrogen atom within these molecules. Thus the larger value of λ for **9**−**12** arises because Cp* is a strong electron donor, creating greater electron density at the metal center and within the M−H bonds. The results obtained by fitting the experimental data to the two-dimensional quantum mechanical exchange coupling model are shown in Table 7.

The calculated frequencies (ν), expressed as wave numbers in Table 7, are believed to describe the H_A-Ir-H_B vibrational wag mode which allows movement along the H_A-H_B internuclear vector. The values for ν decrease as the basicity of L decreases, leading to an increase in J_{ex}. Presumably a lower ν corresponds to less stiff M−H bonds, allowing greater delocalization and overlap for quantum mechanical exchange coupling. The values of ν for **9**−**12** are smaller than those for **13**−**17**. It was expected that the values of ν for **9**−**12** would in fact be larger since the corresponding values for J_{ex} are smaller than those for **13**−**17**. However if $\lambda = 1.1$ Å, and the values of ν for **9**−**12** were larger than those for **13**−**17**, the corresponding values of J_{ex} for **9**−**12** would be too small to detect. While the exchange coupling interaction in **9**−**12** would not necessarily be quenched, the small changes in J_{AB} with temperature would be difficult to observe by ^{1}H NMR spectroscopy. Therefore it appears that the variation in the magnitudes of J_{ex} are not due solely to the differences in ν from complex to complex. Rather the effect of the electron density at the metal center on exchange coupling must be modeled with two adjustable parameters, λ and ν, to accurately fit the experimental data.

The parameter a for **15** has been reported to be 1.686 Å based on neutron diffraction data.[7] The values of a obtained by computer fitting the J_{ex} versus temperature data for **9**−**17** are comparable. The value of 1.69 Å obtained in this manner for **15** was calculated independently during the computer fitting process and was not preset according to the known experimental value. Based on the neutron diffraction study of **15** it was structurally characterized as a capped square pyramid.[7] The hydride distances from the neutron structure for **15** agree with hydride distances determined for **16** by solid state ^{1}H NMR spectroscopy.[8] The complexes **9**−**17** are believed to have essentially the same structures. Thus it was expected that there would be little variation in the H_A-H_B internuclear distances for these complexes.

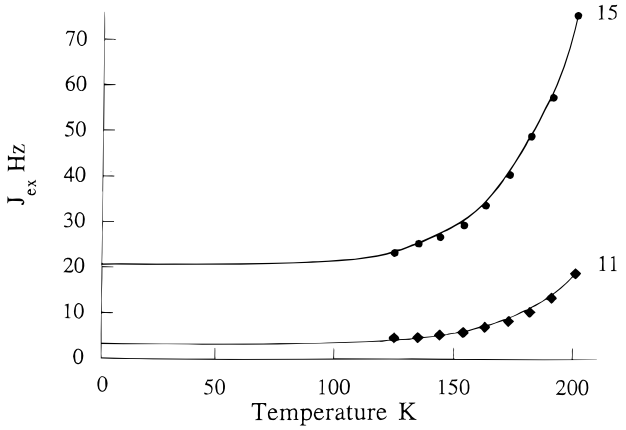

Figure 3. Comparison of the calculated fits to the experimental J_{ex} versus temperature data for **11** and **15**. Calculated fits were extrapolated from 125 to 0 K.

The derived values for λ vary 20% and the derived values for ν vary from 8−10% between the two hydride systems **9**−**12** and **13**−**17**. However the values for a do not vary appreciably between the two systems. Thus the variation in the magnitude of exchange coupling from **9**−**12** to **13**−**17** is apparently caused by differences in λ and ν, which are attributed to the differences in Cp* versus Cp. Within each family **9**−**12** and **13**−**17**, the variation in the magnitude of J_{ex} is caused by differences in ν and a which vary 2−3% depending on the ligand L.

After fitting the J_{ex} versus temperature data, the corresponding fits were extrapolated to 0 K to simulate a situation where zero point motion would be the only contribution to quantum mechanical exchange coupling. In all cases the values determined for J_{ex} at 0 K were nonzero ranging from 0.5−76 Hz. Computer fit extrapolations of the J_{ex} versus temperature data for **11** and **15** are shown in Figure 3. Since the values of J_{ex} at 0 K for **9**−**17** do not converge, the variability of the magnitude of exchange coupling appears to be a ground state effect. A variation in the fundamental vibrational frequencies, describing the potential energy wells for sites A and B in each complex would account for this. The magnitudes for J_{ex} at 0 K suggest that quantum mechanical exchange coupling is a sizable interaction in the ground state. This agrees with the observations for quantum mechanical exchange coupling of ^{3}He/^{4}He at 4 K.[20] The large zero point vibrational amplitude of ^{3}He atoms about their lattice sites corresponds to significant delocalization of their spatial wave functions. This delocalization gives rise to very large quantum mechanical exchange coupling interactions.

If the exchange couplings in **9**−**17** were due to rotational tunneling in a thermally accessible dihydrogen complex, the value of J_{ex} at 0 K should be zero in all cases.[22] At 0 K the equilibrium postulated earlier would completely favor the hydride, as the ground state structure. Therefore no rotational tunneling would occur, and any quantum mechanical exchange interaction would be quenched.

Isotope Effects on Quantum Mechanical Exchange Coupling. As seen in Table 4, the observed J_{AB} for the $Ir(H)_2D$ isotopomer is larger than the J_{AB} for the $Ir(H)_3$ isotopomer for

(40) Weiner, S. J.; Kollman, P. A.; Case, D. A.; Singh, U. C.; Ghio, C.; Alagona, G.; Profeta, S., Jr.; Weiner, P. *J. Am. Chem. Soc.* **1984**, *106*, 765−784.

(41) Levine, I. N. *Physical Chemistry*, 3rd ed.; McGraw-Hill: New York, 1988; pp 807−854.

13−**17**. This difference represents an increase in J_{ex} of 4−8% for the deuterated isotopomers. While the magnitude of this increase in J_{ex} varies for **13**−**17**, the source of the increase has been identified by computer fitting the J_{ex} versus temperature data for the deuterated species. For **13**−**17** a decrease in ν of approximately 1 cm^{-1} leads to the increase in J_{ex} seen at all temperatures for the deuterated isotopomers. The increases in J_{ex} varying from 4−8% for **13**−**17** are easily detectable in J_{AB} observed by ^1H NMR studies. However for **9**−**12** a decrease in ν of 1 cm^{-1} would correspond to increases in J_{ex} and thus J_{AB} varying from only 0.05−2.0% which could not be accurately detected by current NMR methods. Thus there was no apparent increase in J_{AB} for the deuterated isotopomers of **9**−**12**. Apparently one Ir−H bond being replaced by an Ir−D bond within a molecule slightly affects the adjacent Ir−H bond. Thus a change occurs in the frequency of the H−Ir−H wag mode, which is believed to contribute significantly to quantum mechanical exchange coupling. We have no knowledge of reported vibrational spectroscopy studies aimed at determining the secondary effect on H−M−H wag modes of substituting D at an adjacent M−H site. However extensive IR and Raman studies have been reported for Cp_2MH_2 (M = Mo, W) in which substitution of D to form Cp_2MHD caused a shift in the observed frequency of the M−H deformation modes.[42] This is a primary isotope effect since D is participating in the D−M−H vibrational modes. Also substitution of D to form (η-C_5D_5)MH_2 changed the observed M−H deformation frequencies, which is a secondary isotope effect.[40] In light of these reports, the secondary deuterium isotope effects observed in **13**−**17** seem reasonable.

Similar isotope effects were observed in the ^1H NMR spectra of partially tritiated samples of **13**, **14**, and **16**. Computer fitting of the J_{ex} versus temperature data for these samples has determined that the magnitude of the observed increase in J_{AB} corresponds to a decrease in ν of 2 cm^{-1} in going from the $Ir(H)_3$ species to the corresponding $Ir(H)_2T$ isotopomer This decrease in ν for **13**, **14**, and **16** correlates with an increase in J_{ex} ranging from 6.5−9%. A similar decrease in ν for **9**−**12**, **15**, and **17** would lead to an increase in J_{ex} and thus J_{AB} ranging from 4−11%, which should be detectable by ^1H NMR spectroscopy. However, the amount of tritium incorporation needed to observe the signals corresponding to $Ir(H)_2T$ within ^1H NMR spectra of these compounds is a significant radiation hazard. Therefore an extensive study has not been undertaken due to safety considerations. It is presumed that substitution of an Ir−T bond will affect the adjacent Ir−H bonds in a manner similar to the effect of an Ir−D bond, as examined above for **9**−**17**. Thus it is expected that such a substitution of an Ir−T bond will cause a consistent decrease in ν of 2 cm^{-1} for the H−Ir−H wag mode in each complex, **9**−**17**. Presumably the difference in magnitude of the secondary isotope effect in going from D to T is due to the difference in mass of the isotopes, as observed for isotope effects on stretching frequencies in many organic and organometallic compounds.

If we postulate a trihydride complex in equilibrium with a thermally accessible dihydrogen/hydride complex as the chemical basis for quantum mechanical exchange, then we should consider in detail all possible outcomes of isotopic substitution to form IrH_2D or IrH_2T. The heavy isotope can concentrate in the terminal hydride ligand, not affecting rotational tunneling within the dihydrogen ligand. Thus the exchange couplings would also be largely unaffected. It has been shown that the heavy isotope prefers the terminal hydride bond in iridium complexes of the form $[TpIr(PMe_3)(H_2)H]BF_4$ (Tp = hydridotris(pyrazolyl)borate).[43] Alternatively, the heavy isotope can concentrate in the dihydrogen ligand, considerably diminishing the rotational tunneling process. The exchange coupling effect should then be quenched. If there is no site preference for the heavy isotope, then statistical distribution of the isotope would lower the number of dihydrogen ligands able to participate in appreciable rotational tunneling. Thus the exchange coupling effect should decrease. Therefore it is difficult to explain the *increase* in exchange coupling experimentally observed upon isotopic substitution in **9**−**17**, based on a thermally accessible rotational tunneling model.

It should however be pointed out that these small perturbations of the observed coupling are compatible with the computational work of Lledos and co-workers[22] and the model of Eisenstein and co-workers.[23] In both of these approaches to the problem, the ab initio potential surfaces calculated for the hydride motions would be slightly perturbed by the presence of an adjacent heavy isotope of hydrogen. These models allow the approximate calculation of the temperature dependence of the observed exchange coupling, but the simpler model presented here leads to very good agreement with experimental observations.

Conclusions

The similar systems [(η-C_5H_5)Ir(L)H_3]BF_4 and [(η-C_5Me_5)-Ir(L)H_3]BF_4 (L = various phosphines) have been compared in regard to quantum mechanical exchange coupling of the hydride ligands. Considerable experimental evidence seems to support the two-dimensional quantum mechanical exchange coupling model now proposed for these and similar transition-metal hydride systems. In particular the prediction, based on experimental data, of nonzero values for the exchange couplings at 0 K in these systems, seems to preclude rotational tunneling in a thermally accessible dihydrogen species as the means of quantum mechanical exchange coupling. The data obtained make it seem likely that the quantum mechanical exchange coupling interaction in these systems is mediated by a vibrational motion. In addition, no evidence has been seen for a dihydrogen-like transition state for the thermally activation hydride rearrangement which is detected by ^1H NMR above 220 K.

Acknowledgment is made to the National Science Foundation for support of this research. J. D. Close thanks the National Science Foundation (Grant no. CHE-9015765) and the Alexander von Humboldt Stifung for financial support during the course of this work.

JA952142C

(42) Girling, R. B.; Grebenik, P.; Perutz, R. N. *Inorg. Chem.* **1986**, *25*, 31−36.

(43) Heinekey, D. M.; Oldham, W. J., Jr. *J. Am. Chem. Soc.* **1994**, *116*, 3137−3138.